Eur. Phys. J. C (2019) 79:913
https://doi.org/10.1140/epjc/s10052-019-7431-y

THE EUROPEAN PHYSICAL JOURNAL C

Regular Article - Theoretical Physics

Limits on the charged Higgs parameters in the two Higgs doublet model using CMS $\sqrt{s} = 13$ TeV results

Prasenjit Sanyal[a]

Department of Physics, Indian Institute of Technology Kanpur, Kanpur 208 016, India

Received: 3 July 2019 / Accepted: 25 October 2019 / Published online: 11 November 2019

Abstract The latest CMS results on the upper limits on $\sigma_{H^\pm}\text{BR}(H^\pm \to \tau^\pm\nu)$ and $\sigma_{H^\pm}\text{BR}(H^+ \to t\bar{b})$ for $\sqrt{s} = 13$ TeV at an integrated luminosity of 35.9 fb^{-1} are used to impose constraints on the charged Higgs $H^\pm$ parameters within the Two Higgs Doublet Model (2HDM). The 2HDM is the simplest extension of the Standard Model (SM) under the same gauge symmetry to contain charged Higgs and is relatively little constrained compared to the Minimal Supersymmetric Standard Model (MSSM). The latest results lead to much more stringent constraints on the charged Higgs parameter space than for the earlier 8 TeV results. The CMS collaboration also studied the exotic bosonic decays $H^\pm \to W^\pm A$ and $A \to \mu^+\mu^-$ for the first time and put upper limits on the $\text{BR}(t \to H^+b)$ for the light charged Higgs boson. These constraints lead to the exclusion of parameter space which is not excluded by the $\tau\nu$ channel. For comparison the exclusion regions from flavor physics constraints are also discussed.

1 Introduction

The Standard Model (SM) of particle physics is the most successful model in explaining nearly all particle physics phenomenology. The discovery of a neutral scalar of mass 125 GeV with properties similar to the Higgs boson in SM [1–4] makes SM the most acceptable model of particle physics. Despite being successful, the SM fails to explain the existence of dark matter, neutrino oscillations and the matter–antimatter asymmetry. SM also does not explain the mass hierarchy in elementary particles and gravity is not included. Apart from that, there is no fundamental reason to have only one Higgs doublet (i.e. minimal under the SM gauge symmetry) and the discovery of another scalar boson (neutral or charged) would require an extension of the SM. The simplest extension of SM under the same (SM) gauge symmetry is the Two Higgs Doublet Model (2HDM) [5–11]. So far there is no evidence for any other scalar up to a mass of a few TeV and hence the parameter space of 2HDM is getting significantly constrained by experimental observations [12–30]. The scalar sector of 2HDM consists of five scalars, two CP even scalars (h and H), one CP odd scalar (or pseudoscalar) A and two charged Higgs $H^\pm$. The most general Yukawa sector (Type III) of 2HDM leads to flavor changing neutral currents (FCNCs) at tree level. To avoid the FCNC, Glashow and Weinberg implemented a discrete symmetry in the Yukawa sector which leads to four possible types of Yukawa interactions in 2HDM, i.e., Type I, Type II, Type X (lepton specific) and Type Y (flipped model). A brief review on 2HDM is given in Sect. 2.

The production of a charged Higgs particle, depending on its mass with respect to the top quark, can be divided into light ($M_{H^\pm} \ll M_t$), intermediate ($M_{H^\pm} \sim M_t$) and heavy ($M_{H^\pm} \gg M_t$) scenarios [31–34]. Throughout the analysis the alignment limit is considered i.e. $\sin(\beta - \alpha) \to 1$ (where the mixing angles β and α are defined in Sect. 2), so that the neutral scalar h behaves like the SM Higgs boson. The precisely measured electroweak parameter T is highly sensitive on the mass splitting of $H^\pm$, H and A. The alignment limit and minimum mass splitting restricts the charged Higgs decay mostly into the fermionic sector and the experimental constraints put an exclusion bound on the charged Higgs ($M_{H^\pm}$–$\tan\beta$) parameter space. In this paper the 13 TeV CMS results [35–37] at an integrated luminosity of 35.9 fb^{-1} are used to restrict the charged Higgs parameter space as discussed in Sect. 4. Throughout the paper, the notation $H^\pm \to \tau^\pm\nu$ is used for both $H^+ \to \tau^+\nu$ and $H^- \to \tau^-\bar{\nu}$ (similarly for the tb channel). For the charged Higgs production cross section, $\sigma_{H^\pm}$ denotes the sum of σ_{H^+} and σ_{H^-}. A comparison of exclusion limits on charged Higgs parameter space from 13 TeV and 8 TeV CMS results is presented in Sect. 4 along with the indirect flavor physics constraint coming from $B \to X_s\gamma$. As mentioned before, the bosonic decays of a charged Higgs boson into $W^\pm h$, $W^\pm H$ and $W^\pm A$

[a] e-mail: psanyal@iitk.ac.in

are highly suppressed due to the alignment limit and the limited phase space. But once the bosonic decay channel is open, the bounds coming from the $H^{\pm} \to \tau^{\pm}\nu$ and $H^{+} \to t\bar{b}$ become weak [38,39]. In this paper, the latest result from the CMS collaboration [37] is used in the Type I scenario in the mass range $M_{H^{\pm}} \in [100, 160]$ GeV, where the mass splitting $M_{H^{\pm}} - M_A = 85$ GeV and $M_{H^{\pm}} \sim M_H$ is still allowed by the T parameter constraint.

2 Two Higgs doublet model (2HDM) review

For 2HDM, the most general scalar potential [7] is

$$\begin{aligned}\mathcal{V}(\Phi_1, \Phi_2) &= m_{11}^2 \Phi_1^\dagger \Phi_1 + m_{22}^2 \Phi_2^\dagger \Phi_2 - [m_{12}^2 \Phi_1^\dagger \Phi_2 + \text{h.c.}] \\ &+ \frac{1}{2}\lambda_1 (\Phi_1^\dagger \Phi_1)^2 + \frac{1}{2}\lambda_2 (\Phi_2^\dagger \Phi_2)^2 \\ &+ \lambda_3 (\Phi_1^\dagger \Phi_1)(\Phi_2^\dagger \Phi_2) + \lambda_4 (\Phi_1^\dagger \Phi_2)(\Phi_2^\dagger \Phi_1) \\ &+ \left[\frac{\lambda_5}{2}(\Phi_1^\dagger \Phi_2)^2 + h.c.\right] \end{aligned} \tag{1}$$

where $\Phi_{1,2}$ are two isospin doublets with hypercharge $Y = 1/2$. To avoid tree level FCNC the $\mathcal{Z}_2$ symmetry is imposed under which $\Phi_1 \to \Phi_1$ and $\Phi_2 \to -\Phi_2$. This symmetry is softly broken by the parameter $m_{12} \neq 0$. The parameters m_{12} and λ_5 are considered real assuming CP invariance. The two Higgs doublets are parameterized as

$$\Phi_i = \begin{pmatrix} \phi_i^+ \\ \frac{v_i + \rho_i + i\eta_i}{\sqrt{2}} \end{pmatrix} \tag{2}$$

where $\langle \rho_1 \rangle = v_1$, $\langle \rho_2 \rangle = v_2$, $\tan\beta = v_2/v_1$ and $v = \sqrt{v_1^2 + v_2^2} \approx 246$ GeV.

The physical mass eigenstates are given by

$$\begin{aligned}\begin{pmatrix} G^{\pm} \\ H^{\pm} \end{pmatrix} &= R(\beta) \begin{pmatrix} \phi_1^{\pm} \\ \phi_2^{\pm} \end{pmatrix}, \\ \begin{pmatrix} G \\ A \end{pmatrix} &= R(\beta) \begin{pmatrix} \eta_1 \\ \eta_2 \end{pmatrix}, \\ \begin{pmatrix} H \\ h \end{pmatrix} &= R(\alpha) \begin{pmatrix} \rho_1 \\ \rho_2 \end{pmatrix}. \end{aligned} \tag{3}$$

Here $G^{\pm}$ and G are the Nambu–Goldstone bosons that are eaten as the longitudinal components of the massive gauge bosons. The rotation matrix is given by

$$R(\theta) = \begin{pmatrix} \cos\theta & \sin\theta \\ -\sin\theta & \cos\theta \end{pmatrix}. \tag{4}$$

Minimization of the scalar potential in Eq. (1) gives

$$\begin{aligned} m_{11}^2 &= m_{12}^2 \tan\beta - \frac{v_1^2\lambda_1}{2} - \frac{v_2^2\lambda_{345}}{2}, \\ m_{22}^2 &= m_{12}^2 \tan^{-1}\beta - \frac{v_2^2\lambda_2}{2} - \frac{v_1^2\lambda_{345}}{2}, \end{aligned} \tag{5}$$

where $\lambda_{345} = \lambda_3 + \lambda_4 + \lambda_5$. The parameters λ_i written in terms of the physical parameters $M_{H^{\pm}}, M_A, M_H, M_h, m_{12}$ and the mixing angles α and β ($\tan\beta = v_2/v_1$) are

$$\begin{aligned} \lambda_1 &= \frac{M_H^2 R(\alpha)_{11}^2 v_1 + M_h^2 R(\alpha)_{12}^2 v_1 - m_{12}^2 v_2}{v_1^3}, \\ \lambda_2 &= \frac{M_H^2 R(\alpha)_{21}^2 v_2 + M_h^2 R(\alpha)_{22}^2 v_2 - m_{12}^2 v_1}{v_2^3}, \\ \lambda_3 &= \frac{M_H^2 R(\alpha)_{11} R(\alpha)_{21} + M_h^2 R(\alpha)_{12} R(\alpha)_{22}}{v_1 v_2} \\ &\quad + \frac{m_{12}^2 - v_1 v_2 \lambda_{45}}{v_1 v_2}, \\ \lambda_4 &= \frac{m_{12}^2}{v_1 v_2} + \frac{M_A^2}{v^2} - \frac{2M_{H^{\pm}}^2}{v^2}, \\ \lambda_5 &= \frac{m_{12}^2}{v_1 v_2} - \frac{M_A^2}{v^2}, \end{aligned} \tag{6}$$

where $\lambda_{45} = \lambda_4 + \lambda_5$.

The most general Yukawa Lagrangian under the $\mathcal{Z}_2$ symmetry is

$$\begin{aligned} \mathcal{L}_{\text{Yukawa}}^{\text{2HDM}} &= -\bar{Q}_L Y_u \tilde{\Phi}_u u_R - \bar{Q}_L Y_d \Phi_d d_R \\ &\quad - \bar{L} Y_l \Phi_l l_R + h.c. \end{aligned} \tag{7}$$

where $\Phi_f (f = u, d \text{ or } l)$ is either Φ_1 or Φ_2, depending on the Yukawa models of 2HDM. The four possible $\mathcal{Z}_2$ charge assignments of the quarks and charged leptons are summarized in Table 1.

Table 1 Charge assignment under $\mathcal{Z}_2$ symmetry to avoid FCNC at tree level

Model	Φ_1	Φ_2	u_R	d_R	l_R	Q_L, L_L
Type I	+	−	−	−	−	+
Type II	+	−	−	+	+	+
Type X	+	−	−	−	+	+
Type Y	+	−	−	+	−	+

In Type I 2HDM, the second Higgs doublet Φ_2 couples to the fermions, so all the quarks and charged leptons get their masses from the VEV of Φ_2 (ie. v_2). In Type II 2HDM, up-type quarks couple to Φ_2 whereas down-type quarks and charged leptons couple to Φ_1. Hence in Type II up-type quarks get masses from v_2 and down-type quarks and charged leptons get masses from v_1. The Higgs sector of the Minimal Supersymmetric Standard Model (MSSM) is a special 2HDM whose Yukawa interaction is of Type II. For Type X (also called the Lepton Specific Model), the quark sector is similar to Type I but the charged leptons are coupled to Φ_1 and finally in the Type Y (also called the Flipped Model) the quark sector is similar to Type II but the leptons are coupled

Table 2 Choices of the couplings ξ_f for the four Yukawa models of 2HDM

Model	ξ_d	ξ_u	ξ_l
Type I	$\cot\beta$	$\cot\beta$	$\cot\beta$
Type II	$-\tan\beta$	$\cot\beta$	$-\tan\beta$
Type X	$\cot\beta$	$\cot\beta$	$-\tan\beta$
Type Y	$-\tan\beta$	$\cot\beta$	$\cot\beta$

to Φ_2. Among them, Type II 2HDM has been most widely investigated because of its resemblance with MSSM.

The Yukawa interactions of $H^\pm$ with quarks and leptons take the form

$$\mathcal{L}_Y = -\frac{\sqrt{2}}{v} H^+ \bar{u}[\xi_d V M_d P_R - \xi_u M_u V P_L]d - \frac{\sqrt{2}}{v} H^+ \xi_l \bar{\nu} M_l P_R l \quad (8)$$

where V is the CKM matrix and $P_{R,L} = \frac{1}{2}(1 \pm \gamma_5)$ are the chirality projection operators (Table 2).

3 $H^\pm$ production and decay channels

The production cross section of the charged Higgs particle depends on its mass with respect to top quark and can be classified into three categories. The light charged Higgs scenario is defined by the mass of charged Higgs being light enough ($M_{H^\pm} \lesssim 150$ GeV) such that the on-shell decay of the top quark, $t \to H^+ b$, is allowed. The production cross section for the light scenario is simply given by the product of top pair production (double-resonant mode), $pp \to t\bar{t}$, times the branching fraction of the top into charged Higgs, $t \to H^+ b$. The $pp \to t\bar{t}$ cross section has been computed at NNLO in QCD including resummation of NNLL soft gluon terms using the code Top++2.0 [40]. The heavy charged Higgs scenario is defined for $M_{H^\pm} \gtrsim 200$ GeV where the charged Higgs mass is sufficiently large compared to top quark. In this scenario, the dominant charged Higgs production channel is the associated production with a top quark (single-resonant mode) $pp \to tbH^\pm$. The production cross section for the heavy charged Higgs boson is computed in the 4FS and 5FS schemes in Refs. [32,33], and combined to obtain the total cross section using the Santander matching scheme [41] for different values of $\tan\beta$.[1] The intermediate charged Higgs scenario is considered for $M_{H^\pm}$ close to top quark i.e. $150 \lesssim M_{H^\pm} \lesssim 200$ GeV. In this region, the non-resonant top quark production mode also contributes along with the single-resonant and double-resonant modes. Cross sections at NLO QCD accuracy in the 4FS scheme as given in Ref. [31] are considered. Figure 1 shows the leading order (LO) diagrams of charged Higgs production in the three scenarios.[2] Since the $H^\pm$ interaction to the quark sector of Type I and Type X and similarly that for Type II and Type Y are the same, the production cross sections in different models are related by $\sigma^{H^\pm}_{\text{Type I}} = \sigma^{H^\pm}_{\text{Type X}}$ and $\sigma^{H^\pm}_{\text{Type II}} = \sigma^{H^\pm}_{\text{Type Y}}$.

For the case of charged Higgs fermionic decays, in Type I all the fermionic couplings are proportional to $\cot\beta$ and hence the branching fractions are independent of $\tan\beta$. The

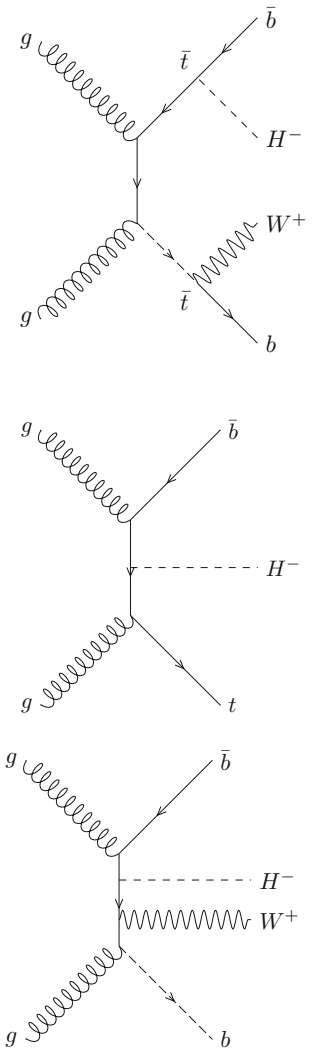

Fig. 1 Leading order (LO) diagrams for the charged Higgs particle are shown. The double-resonant top pair production (top diagram) is the dominant process for light $H^\pm$. The single-resonant top quark production (middle diagram) is dominant for heavy $H^\pm$. In the intermediate $H^\pm$ scenario ($M_{H^\pm} \sim M_t$), both of these production channels along with the non-resonant top quark production (bottom diagram) are taken into account

[1] Since the charged Higgs production cross sections scales with the glue–glue luminosity, in the mass range of 200–600 GeV, the production cross section increases by a factor of 4–6 from 8 to 13 TeV.

[2] The cross sections are provided in https://twiki.cern.ch/twiki/bin/view/LHCPhysics/LHCHXSWGMSSMCharged .

$\tau\nu$ channel is the dominant decay channel for light charged Higgs in Type I. However, for heavy charged Higgs scenario in Type I, the Br($H^\pm \to \tau\nu$) is suppressed by M_τ^2/M_t^2 over Br($H^+ \to t\bar{b}$), leading to nearly 100% branching fraction in the $t\bar{b}$ channel. In Type II and Type X the lepton sector coupling to $H^\pm$ being proportional to $\tan\beta$, the decay into $\tau\nu$ is dominant for light $H^\pm$ and quite sizable for heavy $H^\pm$ for $\tan\beta \gtrsim 1$. As seen in Fig. 2 for heavy $H^\pm$ scenario in Type X, the $H^\pm$ branching fraction to $\tau\nu$ starts to dominate over the $t\bar{b}$ channel for large $\tan\beta$. In Type Y, because of the $\cot\beta$ dependence in the lepton sector the $\tau\nu$ channel gets suppressed compared to the hadronic decay modes (dominantly into $t\bar{b}$ for heavy $H^\pm$). The branching fractions computed using the public code HDECAY [42,43] are shown in Fig. 2 for $M_{H^\pm} = 250$ GeV, for all Yukawa types of 2HDM. The code HDECAY also includes the three-body decay of the charged Higgs particle, i.e., $H^+ \to t^*\bar{b} \to W^+ b\bar{b}$ below the two-body decay threshold of $H^+ \to t\bar{b}$ mode [44]. Note that the branching fraction of $H^\pm$ into the fermionic sector is given for situations where there are no $H^\pm$ decays into the neutral scalars.

Apart from the fermionic decays, $H^\pm$ can also decay to $W^\pm$ and neutral scalars h, H or A. The couplings to $W^\pm$ and neutral scalars are (all fields are incoming)

$$
\begin{aligned}
H^\mp W^\pm h &: \frac{\mp ig}{2}\cos(\beta-\alpha)(p_\mu - p_\mu^\mp),\\
H^\mp W^\pm H &: \frac{\mp ig}{2}\sin(\beta-\alpha)(p_\mu - p_\mu^\mp),\\
H^\mp W^\pm A &: \frac{g}{2}(p_\mu - p_\mu^\mp),
\end{aligned}
\tag{9}
$$

where p_μ and $p_\mu^\mp$ are the momenta of the neutral and charged scalars. In the alignment limit $\sin(\beta-\alpha) \to 1$ (which is considered throughout the paper) $H^\pm$ decay to h is suppressed. The decays into the H and A channels depend on the mass splitting allowed by the T parameter. In the generic 2HDM, there are no mass relations between $H^\pm$, H and A unlike MSSM and for some parameter choice, the bosonic decays can be more dominant over the fermionic decays once the channels are open.

4 Experimental constraints

The theoretical constraints of 2HDM consist of vacuum stability [45,46], perturbative unitarity [47,48] and tree level unitarity [49–51]. The Electro-Weak Precision Observables (EWPOs) $S(0.05\pm0.11)$, $T(0.09\pm0.13)$ and $U(0.01\pm0.11)$ [52,53], specially the T parameter [54], restrict the mass splitting of $H^\pm$, H and A. In this paper, $M_{H^\pm} = M_H = M_A$ is considered to impose the exclusion limits from the $H^\pm \to \tau^\pm\nu$ and $H^+ \to t\bar{b}$ channels over the mass range $M_{H^\pm} \in [80, 2000]$ GeV. Perturbative unitarity for a wide

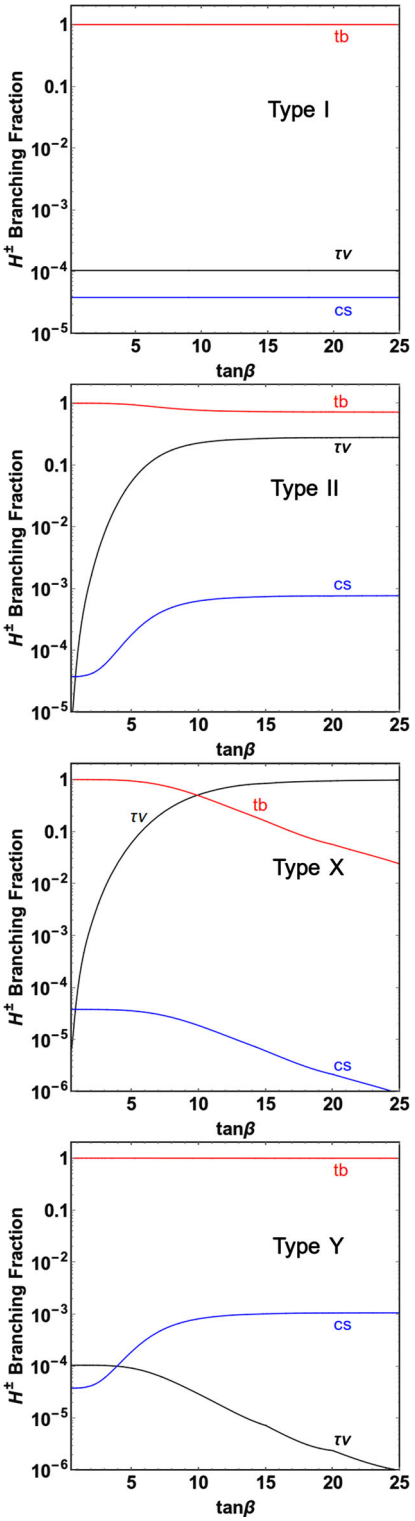

Fig. 2 Branching fractions of the charged Higgs particle into the dominant fermionic sectors as a function of $\tan\beta$ for $M_{H^\pm} = 250$ GeV. The alignment limit $\sin(\beta-\alpha) \to 1$ and degenerate $M_{H^\pm}$, M_H and M_A are considered to prevent $H^\pm \to W^\pm\phi$ ($\phi = h, H, A$) and satisfy the T parameter constraint

region of tan β can be satisfied by a proper choice of the soft $\mathcal{Z}_2$ breaking parameter, $m_{12}^2 = M_A^2 \sin\beta\cos\beta$. The theoretical constraints are checked using the package 2HDMC- 1.7.0 [55]. The alignment limit $\sin(\beta-\alpha) \to 1$ is the condition most favored by the experimentalists. In this limit the couplings of the neutral scalar h in 2HDM is similar to the SM Higgs boson and can be identified with the observed 125 GeV Higgs boson. In the alignment limit the other CP even scalar, H, behaves as gauge-phobic i.e. its coupling to the gauge bosons $W^\pm/Z$ is very suppressed. In the context of a charged Higgs analysis for the $H^\pm \to \tau^\pm\nu$ and $H^+ \to t\bar{b}$ channels, the alignment limit is useful as it completely suppresses the $H^\pm \to W^\pm h$ decay. LEP experiments [56] have given limits on the mass of the charged Higgs boson in 2HDM from the charged Higgs searches in Drell–Yan events, $e^+e^- \to Z/\gamma \to H^+H^-$, excluding $M_{H^\pm} \lesssim 80$ GeV (Type II) and $M_{H^\pm} \lesssim 72.5$ GeV (Type I) at 95% confidence level. Among the constraints from B meson decays (flavor physics constraints), the $B \to X_s\gamma$ decay [57] puts a very strong constraint on Type II and Type Y 2HDM, excluding $M_{H^\pm} \lesssim 580$ GeV and almost independently of tan β. For Type I and Type X, the $B \to X_s\gamma$ constraint is sensitive only for low tan β. So for $M_H^\pm \lesssim 580$ GeV, Type II and Type Y are not considered further.

The LHC experiments have already set limits on the $M_{H^\pm}$–tan β plane using $\sqrt{s} = 8$ TeV observations from the $H^\pm \to \tau^\pm\nu$ [58,59] and $H^+ \to t\bar{b}$ [59,60] channels. For $M_{H^\pm} \in [80, 160]$ GeV, the most important constraint comes from the $H^\pm \to \tau^\pm\nu$ channel.[3] The exclusion regions are shown with green colors in Fig. 3 using the 8 TeV CMS results at an integrated luminosity of 19.7 fb^{-1} for Type I and Type X. In Type X the leptonic coupling being proportional to tan β excludes a slightly larger region of tan β. Using the upper bounds on the $\sigma_{H^\pm}\text{BR}(H^\pm \to \tau^\pm\nu)$ from the latest CMS results [35] for $\sqrt{s} = 13$ TeV at an integrated luminosity of 35.9 fb^{-1}, a much larger region of tan β is excluded as shown in red colors in Fig. 3 for both Type I and Type X. Just above $M_{H^\pm} = 160$ GeV tan $\beta \lesssim 1$ is allowed by this channel in the Type X model. This is because the exclusion in Type X at low tan β is less severe than Type I.

For $M_{H^\pm}$ greater than the top quark mass, the constraint coming from the $\tau\nu$ channel does not put any significant bound on the $M_{H^\pm}$–tan β parameter space. Therefore in the higher mass range the $H^+ \to t\bar{b}$ channel has to be studied. The tb channel, unlike the $\tau\nu$ channel, is not clean enough and suffers from various QCD backgrounds, but sophisticated analysis is used to study the tb channel in both 8 TeV and 13 TeV by the CMS collaboration. The CMS 8 TeV upper limit on $\sigma(pp \to t(b)H^+)$ assuming $\text{BR}(H^+ \to t\bar{b}) = 100\%$ [59] restricts the parameter space for $200 < M_{H^\pm} < 600$ GeV. The exclusion region using the 8 TeV results are shown in green colors in Fig. 4 for Type I. A recent paper from the CMS collaboration [36] for $\sqrt{s} = 13$ TeV and 35.9 fb^{-1} puts an upper limit at 95% CL on $\sigma_{H^\pm}\text{BR}(H^+ \to t\bar{b})$ with the single-lepton and dilepton final states combined. The resulting exclusion regions in the $M_{H^\pm}$–tan β plane for heavy charged Higgs $M_{H^\pm} \in [200, 2000]$ GeV in Type I and $M_{H^\pm} \in [600, 2000]$ in Type II are shown in Fig. 4 with red colors. Since the charged Higgs leptonic decay mode in TypeY is much suppressed compared to the $H^+ \to t\bar{b}$ mode and for the Type X scenario, the $H^+ \to t\bar{b}$ mode is dominant for low tan β as shown in Fig. 2 (bottom two plots). The exclusion regions of Type X and Type Y are equivalent to the exclusion regions of Type I and Type II, respectively.

So far, the charged Higgs decay to the gauge boson and neutral scalars $H^\pm \to W^\pm H/A$ are not considered by

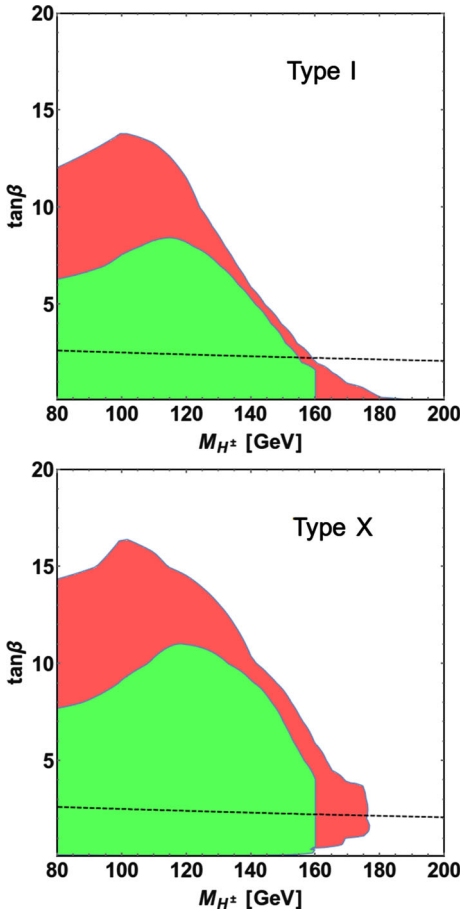

Fig. 3 Exclusion region in Type I and Type X from the upper limits on $\sigma_{H^\pm}BR(H^\pm \to \tau^\pm\nu)$ CMS 13 TeV observations are shown in red color. The green color shows the exclusion region from the upper limits on $\text{BR}(t \to H^+b)\text{BR}(H^\pm \to \tau^\pm\nu)$ CMS 8 TeV observations. The region below the black dashed line is excluded by the $\text{BR}(B \to X_s\gamma)$ constraint

[3] The constraints of charged Higgs bosons decaying in the fermionic sector are useful only when the charged Higgs bosonic decays are suppressed.

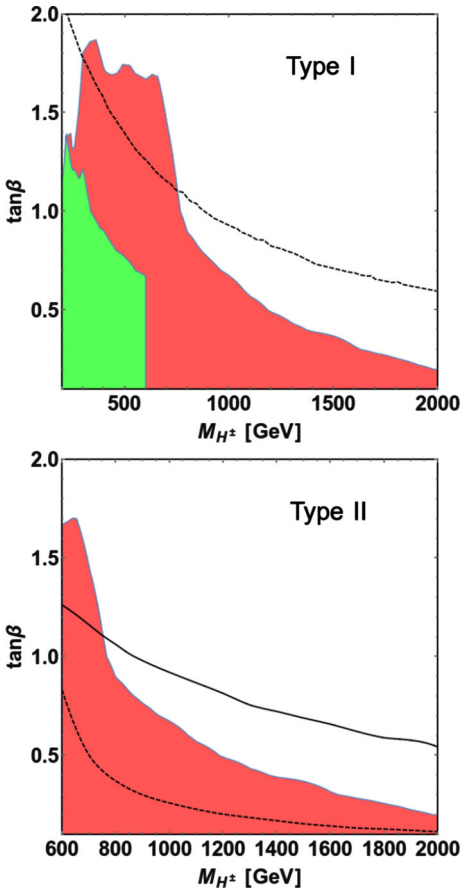

Fig. 4 Exclusion region in Type I and Type II from the upper limits on $\sigma_{H^\pm} BR(H^+ \to t\bar{b})$ CMS 13 TeV observations are shown in red color. The green color (upper plot) shows the exclusion region from the upper limits on $\sigma(pp \to \bar{t}(b)H^+)$ CMS 8 TeV observations assuming $\text{BR}(H^+ \to t\bar{b}) = 1$. The region below the black dashed line is excluded by $\text{BR}(B \to X_s\gamma)$ constraint and the region below the continuous black line in Type II (bottom plot) is excluded by the $\text{BR}(B_s \to \mu^+\mu^-)$ constraint

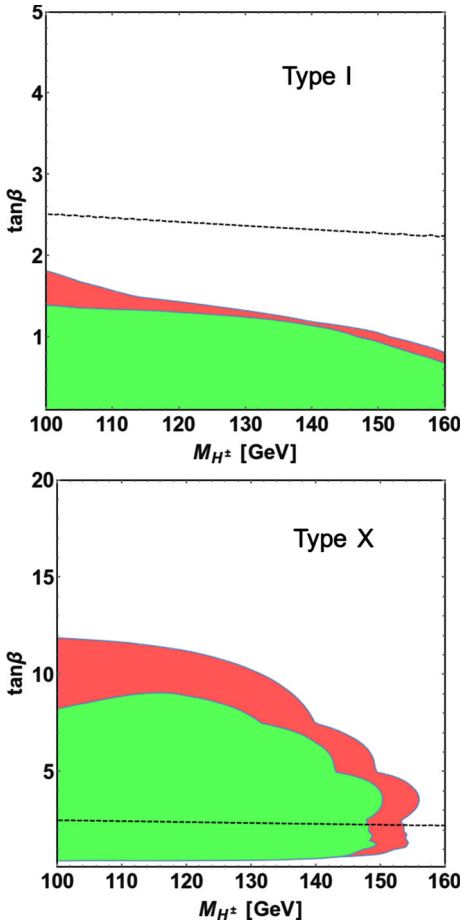

Fig. 5 Exclusion region in Type I and Type X from the upper limits on $\sigma_{H^\pm} BR(H^\pm \to \tau^\pm\nu)$ CMS 13 TeV observations are shown in red color. The green color shows the exclusion region from the upper limits on $\text{BR}(t \to H^+b)\text{BR}(H^\pm \to \tau^\pm\nu)$ CMS 8 TeV observations. The region below the black dashed line is excluded by the $\text{BR}(B \to X_s\gamma)$ constraint. Here the mass difference $M_{H^\pm} - M_A = 85$ GeV for $M_{H^\pm} \in [100, 160]$ GeV and $M_{H^\pm} \sim M_H$ is considered. The exclusion region is less compared to Fig. 3 where the masses of $H^\pm$, H and A are nearly the same

assuming near mass degeneracy of $H^\pm$, H and A. But once the bosonic decays are kinematically allowed, the charged Higgs boson can significantly decay into these channels. Figure 5 shows the exclusion regions coming from the $H^\pm \to \tau^\pm\nu$ channel where the mass difference $M_{H^\pm} - M_A = 85$ GeV is considered for $M_{H^\pm} \in [100, 160]$ GeV and $M_{H^\pm} \sim M_H$. The red regions are excluded by using the upper limits on $\sigma_{H^\pm} BR(H^\pm \to \tau^\pm\nu)$ CMS 13 TeV observations and the green regions are excluded by using the upper limits on $\text{BR}(t \to H^+b)\text{BR}(H^\pm \to \tau^\pm\nu)$ CMS 8 TeV observations. For this choice of the mass difference, the exclusion regions are less than for Fig. 3 because of the significant decay of $H^\pm$ into $W^\pm A$. As mentioned above, in Type X the leptonic coupling being proportional to $\tan\beta$ excludes a larger region than for Type I.

The CMS collaboration [37] recently studied the scenario where the mass difference of $H^\pm$ and A is $\sim$ 85 GeV for $M_{H^\pm} \in [100, 160]$ GeV. The charged Higgs produced in pp collision in LHC at an integrated luminosity of 35.9 fb^{-1} decays dominantly into $W^\pm$ and A with final states $e\mu\mu$ or $\mu\mu\mu$. In this analysis, the CMS assumed $\text{BR}(H^\pm \to W^\pm A) = 1$ and $\text{BR}(A \to \mu^+\mu^-) = 3 \times 10^{-4}$. Also this is the first experimental result in the channel $H^\pm \to W^\pm A$, $A \to \mu^+\mu^-$ at LHC to put upper limits on $\text{BR}(t \to H^+b)$. Such a low branching fraction of $A \to \mu^+\mu^-$ can be realized in Type I 2HDM where $\text{BR}(A \to \mu^+\mu^-) \sim 2.4 \times 10^{-4}$ for $A \in [15, 75]$ GeV and it goes very well with the CMS assumption. The other assumption, $\text{BR}(H^\pm \to W^\pm A) = 1$, is satisfied in Type I scenario when $\tan\beta \geq 1$ as seen in Fig. 6. In Type I scenario the charged Higgs coupling to the fermionic sector being proportional to $\cot\beta$, the assumption $\text{BR}(H^\pm \to W^\pm A) = 1$ starts to fail for $\tan\beta < 1$. The theoretical constraints can be satisfied with a proper

choice of m_{12}^2 and the oblique parameter T can be satisfied by considering $M_{H^\pm} \cong M_H$. The observed upper limits at 95% CL on BR($t \to H^+ b$) for $M_H^\pm \in [100, 160]$ GeV and $M_{H^\pm} - M_A = 85$ GeV with the above assumptions are used to find the exclusion region. In Fig. 6 the red region (above $\tan\beta \geq 1$) shows the exclusion region where we have smoothly fitted the observed CMS upper limit on BR($t \to H^+ b$) in the range of 0.63 to 2.9%. Other 2HDMs like Type II and Type Y are not considered, as for this mass range of charged Higgs Type II and Type Y are ruled out by the $B \to X_s\gamma$ constraint. Unlike Type I where all the fermionic couplings of A are proportional to $\cot\beta$, in Type X the pseudoscalar coupling to the lepton sector is proportional to $\tan\beta$ whereas its coupling to the quark sector is proportional to $\cot\beta$. Thus the BR($A \to \mu^+\mu^-$) increases with $\tan\beta$. The CMS assumption is satisfied in Type X scenario only when $\tan\beta$ is close to 1 and for this situation the theoretically estimated BR($t \to H^+ b$) is the same as in Type I (because of the same coupling) and above the upper limit of the CMS observation. Comparing Figs. 5 and 6, the exclusion regions coming from the $\tau\nu$ channel are weak once the $H^\pm \to W^\pm A$ channel is open. Figure 6 (bottom plot) excludes the regions of parameter space which are not excluded in Fig. 5 (top plot).

For completeness, the indirect constraints from the flavor physics is also considered in the paper as the B meson decay depends strongly on the parameters $M_{H^\pm}$ and $\tan\beta$. The public code SuperIso- 3.7 [61] is used for flavor physics computation. As mentioned above, for Type II and Type Y, a charged Higgs boson lighter than ~ 580 GeV is completely ruled out for a large region of $\tan\beta$ by the BR($B \to X_s\gamma$) constraint [62], which is measured to be $(3.32 \pm 0.15) \times 10^{-4}$ [63]. For Type I (and similarly for Type X) the BR($B \to X_s\gamma$) constraint excludes $\tan\beta \lesssim 2$. In Figs. 3, 4, 5 and 6 the regions below the black dashed lines are excluded by the BR($B \to X_s\gamma$) observation. In Type II (and similarly in Type Y) for $M_{H^\pm}$ above 600 GeV, the rare decay of $B_s \to \mu^+\mu^-$ (the branching fraction of which is measured to be $(3.0 \pm 0.6 \pm 0.25) \times 10^{-9}$) as reported by LHCb collaboration excludes a greater region of parameter space than the $B \to X_s\gamma$ constraint. For the Type II scenario in Fig. 4 the region below the black continuous line is excluded by BR($B_s \to \mu^+\mu^-$) constraint.

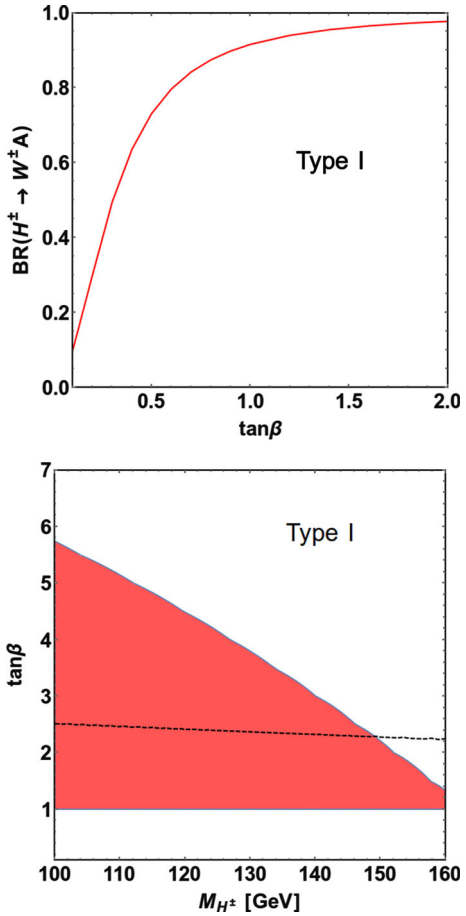

Fig. 6 Branching fraction of $H^\pm \to W^\pm A$ as a function of $\tan\beta$ (upper plot) for $M_{H^\pm} - M_A = 85$ GeV and $M_{H^\pm} = 150$ GeV. The exclusion region (bottom plot) in Type I is shown in red color from the first upper limits on BR($t \to H^+ b$) CMS 13 TeV observations in the charged Higgs decay mode: $H^\pm \to W^\pm A$ and $A \to \mu^+\mu^-$ with the assumptions BR($H^\pm \to W^\pm A$) = 1 and BR($A \to \mu^+\mu^-$) = 3×10^{-4}. For the charged Higgs bosonic decay channel the mass difference $M_{H^\pm} - M_A = 85$ GeV for $M_{H^\pm} \in [100, 160]$ GeV is considered. The region below the black dashed line is excluded by BR($B \to X_s\gamma$) constraint

5 Summary and conclusions

The 2HDM is the simplest extension of SM containing charged Higgs. The two most dominant channels, $H^\pm \to \tau^\pm\nu$ and $H^+ \to t\bar{b}$, for the search of $H^\pm$ are studied using the latest CMS results for $\sqrt{s} = 13$ TeV at an integrated luminosity of 35.9 fb $^{-1}$. The $\tau\nu$ channel excludes a large region of $\tan\beta < \mathcal{O}(15)$ for a charged Higgs mass less than 160 GeV both in Type I and Type X. For a heavy charged Higgs boson, the $\tau\nu$ channel does not lead to any significant constraint on the parameter space. However, in this case, the tb channel excludes a significant range of values of $\tan\beta$ in Type I and II and this behavior is carried over to Type X and Type Y. The exclusion regions obtained from the 13 TeV CMS results are compared with the exclusion regions from 8 TeV CMS results. Exclusion bounds from B meson decays are also discussed for all Yukawa types of 2HDM. The fermionic channels are studied for situations where the exotic decays of a charged Higgs boson into a gauge boson and neutral scalars ($H^\pm \to W^\pm/h/H/A$) are suppressed either by the alignment limit or due to limited phase space. But once the bosonic decay channels are open, they can be the dominant charged Higgs decay channels and the constraints

from $H^{\pm} \to \tau^{\pm}\nu$ and $H^{+} \to t\bar{b}$ will be less restrictive. The CMS collaboration for the first time studied the exotic bosonic decay channel $H^{\pm} \to W^{\pm}A$ and $A \to \mu^{+}\mu^{-}$ to put upper limits on BR($t \to H^{+}b$) for $M_{H^{\pm}} \in [100, 160]$ GeV with a mass splitting of $M_{H^{\pm}} - M_A = 85$ GeV. These results are used to exclude a significant parameter space of the charged Higgs boson in Type I 2HDM which is not excluded by the $\tau\nu$ channel. It is expected that a significant parameter space of the charged Higgs boson will be excluded in all Yukawa types of 2HDM (as well as in MSSM) if these exotic bosonic decay channels of charged Higgs are analyzed by CMS or ATLAS collaborations for various charged Higgs mass ranges.

Acknowledgements The author would like to thank Ravindra K. Verma and Aravind H. Vijay for some useful discussions. The author also acknowledges Pankaj Jain for discussions and useful comments on the paper.

Data Availability Statement This manuscript has no associated data or the data will not be deposited. [Authors' comment: This is a theoretical paper to put constraints on the charged Higgs parameters of two Higgs doublet model based on latest results from CMS.]

Funded by SCOAP[3].

References

1. ATLAS collaboration, G. Aad et al., Observation of a new particle in the search for the Standard Model Higgs boson with the ATLAS detector at the LHC, Phys. Lett. **B716**, 1–29 (2012). arXiv:1207.7214
2. ATLAS collaboration, G. Aad et al., Measurements of Higgs boson production and couplings in diboson final states with the ATLAS detector at the LHC, Phys. Lett. **B726**, 88–119 (2013). arXiv:1307.1427
3. CMS collaboration, S. Chatrchyan et al., Observation of a new boson at a mass of 125 GeV with the CMS experiment at the LHC, Phys. Lett. **B716**, 30–61 (2012). arXiv:1207.7235
4. CMS collaboration, S. Chatrchyan et al., Observation of a New Boson with Mass Near 125 GeV in pp Collisions at $\sqrt{s} = 7$ and 8 TeV, JHEP **06**, 081 (2013). arXiv:1303.4571
5. J.F. Gunion, H.E. Haber, The CP conserving two Higgs doublet model: the approach to the decoupling limit. Phys. Rev. D **67**, 075019 (2003). arXiv:hep-ph/0207010
6. J.F. Gunion, H.E. Haber, G.L. Kane, S. Dawson, The Higgs Hunter's Guide. Front. Phys. **80**, 1–404 (2000)
7. G.C. Branco, P.M. Ferreira, L. Lavoura, M.N. Rebelo, M. Sher, J.P. Silva, Theory and phenomenology of two-Higgs-doublet models. Phys. Rept. **516**, 1–102 (2012). arXiv:1106.0034
8. S. Davidson, H.E. Haber, Basis-independent methods for the two-Higgs-doublet model. Phys. Rev. D **72**, 035004 (2005). arXiv:hep-ph/0504050
9. A. Pich, P. Tuzon, Yukawa alignment in the two-Higgs-doublet model. Phys. Rev. D **80**, 091702 (2009). arXiv:0908.1554
10. J. Bernon, J.F. Gunion, H.E. Haber, Y. Jiang, S. Kraml, Scrutinizing the alignment limit in two-Higgs-doublet models: m_h=125 GeV. Phys. Rev. D **92**, 075004 (2015). arXiv:1507.00933
11. J. Bernon, J.F. Gunion, H.E. Haber, Y. Jiang, S. Kraml, Scrutinizing the alignment limit in two-Higgs-doublet models. II. m_H=125 GeV. Phys. Rev **D93**, 035027 (2016). arXiv:1511.03682
12. M. Aoki, S. Kanemura, K. Tsumura, K. Yagyu, Models of Yukawa interaction in the two Higgs doublet model, and their collider phenomenology. Phys. Rev. D **80**, 015017 (2009). arXiv:0902.4665
13. F. Mahmoudi, O. Stal, Flavor constraints on the two-Higgs-doublet model with general Yukawa couplings. Phys. Rev. D **81**, 035016 (2010). arXiv:0907.1791
14. M. Maniatis, O. Nachtmann, On the phenomenology of a two-Higgs-doublet model with maximal CP symmetry at the LHC. II. Radiative effects. JHEP **04**, 027 (2010). arXiv:0912.2727
15. M. Jung, A. Pich, P. Tuzon, Charged-Higgs phenomenology in the Aligned two-Higgs-doublet model. JHEP **11**, 003 (2010). arXiv:1006.0470
16. C.-Y. Chen, S. Dawson, Exploring two Higgs doublet models through Higgs production. Phys. Rev. D **87**, 055016 (2013). arXiv:1301.0309
17. C.-W. Chiang, K. Yagyu, Implications of Higgs boson search data on the two-Higgs doublet models with a softly broken Z_2 symmetry. JHEP **07**, 160 (2013). arXiv:1303.0168
18. B. Coleppa, F. Kling, S. Su, Constraining type II 2HDM in light of LHC Higgs searches. JHEP **01**, 161 (2014). arXiv:1305.0002
19. C.-Y. Chen, S. Dawson, M. Sher, Heavy Higgs searches and constraints on two Higgs doublet models. Phys. Rev. D **88**, 015018 (2013). arXiv:1305.1624
20. P. Bechtle, S. Heinemeyer, O. Stal, T. Stefaniak, G. Weiglein, Applying exclusion likelihoods from LHC searches to extended Higgs sectors. Eur. Phys. J. C **75**, 421 (2015). arXiv:1507.06706
21. V. Keus, S.F. King, S. Moretti, K. Yagyu, CP violating two-Higgs-doublet model: constraints and LHC predictions. JHEP **04**, 048 (2016). arXiv:1510.04028
22. A.G. Akeroyd et al., Prospects for charged Higgs searches at the LHC. Eur. Phys. J. C **77**, 276 (2017). arXiv:1607.01320
23. G. Cacciapaglia, A. Deandrea, S. Gascon-Shotkin, S. Le Corre, M. Lethuillier, J. Tao, Search for a lighter Higgs boson in Two Higgs Doublet Models. JHEP **12**, 068 (2016). arXiv:1607.08653
24. M. Krawczyk, S. Moretti, P. Osland, G. Pruna, R. Santos, Prospects for 2HDM charged Higgs searches. J. Phys. Conf. Ser. **873**, 012048 (2017). arXiv:1703.05925
25. A. Arbey, F. Mahmoudi, O. Stal, T. Stefaniak, Status of the charged Higgs Boson in two Higgs doublet models. Eur. Phys. J. C **78**, 182 (2018). arXiv:1706.07414
26. A. Arhrib, R. Benbrik, H. Harouiz, S. Moretti, A. Rouchad, A guidebook to hunting charged Higgs Bosons at the LHC. arXiv:1810.09106
27. D. Bhatia, U. Maitra, S. Niyogi, Discovery prospects of a light Higgs boson at the LHC in type-I 2HDM. Phys. Rev. D **97**, 055027 (2018). arXiv:1704.07850
28. S. Gori, H.E. Haber, E. Santos, High scale flavor alignment in two-Higgs doublet models and its phenomenology. JHEP **06**, 110 (2017). arXiv:1703.05873
29. A. Arhrib, R. Benbrik, R. Enberg, W. Klemm, S. Moretti, S. Munir, Identifying a light charged Higgs boson at the LHC Run II. Phys. Lett. B **774**, 591–598 (2017). arXiv:1706.01964
30. L. Barak, Search for charged higgs bosons with the atlas detector. Nucl. Particle Phys. Proc. **273–275**, 896–900 (2016)
31. C. Degrande, R. Frederix, V. Hirschi, M. Ubiali, M. Wiesemann, M. Zaro, Accurate predictions for charged Higgs production: closing the $m_{H^{\pm}} \sim m_t$ window. Phys. Lett. B **772**, 87–92 (2017). arXiv:1607.05291

32. M. Flechl, R. Klees, M. Kramer, M. Spira, M. Ubiali, Improved cross-section predictions for heavy charged Higgs boson production at the LHC. Phys. Rev. D **91**, 075015 (2015). arXiv:1409.5615
33. C. Degrande, M. Ubiali, M. Wiesemann, M. Zaro, Heavy charged Higgs boson production at the LHC. JHEP **10**, 145 (2015). arXiv:1507.02549
34. LHC Higgs Cross Section Working Group collaboration, D. de Florian et al., Handbook of LHC Higgs cross sections: 4. Deciphering the nature of the Higgs sector. arXiv:1610.07922
35. CMS collaboration, A.M. Sirunyan et al., Search for charged Higgs bosons in the $H^{\pm} \to \tau^{\pm}\nu_{\tau}$ decay channel in proton-proton collisions at $\sqrt{s} = 13$ TeV, arXiv:1903.04560
36. CMS collaboration, C. Collaboration, Search for a charged Higgs boson decaying into top and bottom quarks in proton-proton collisions at 13 TeV in events with electrons or muons
37. CMS collaboration, A.M. Sirunyan et al., Search for a light charged Higgs boson decaying to a W boson and a CP-odd Higgs boson in final states with $e\mu\mu$ or $\mu\mu\mu$ in proton-proton collisions at $\sqrt{s} =$ 13 TeV, arXiv:1905.07453
38. F. Kling, A. Pyarelal, S. Su, Light charged higgs bosons to AW/HW via top decay. JHEP **11**, 051 (2015). arXiv:1504.06624
39. B. Coleppa, F. Kling, S. Su, Charged Higgs search via $AW^{\pm}/HW^{\pm}$ channel. JHEP **12**, 148 (2014). arXiv:1408.4119
40. M. Czakon, A. Mitov, Top++: a program for the calculation of the top-pair cross-section at hadron colliders. Comput. Phys. Commun. **185**, 2930 (2014). arXiv:1112.5675
41. R. Harlander, M. Kramer, M. Schumacher, Bottom-quark associated Higgs-boson production: reconciling the four- and five-flavour scheme approach. arXiv:1112.3478
42. A. Djouadi, J. Kalinowski, M. Spira, HDECAY: A Program for Higgs boson decays in the standard model and its supersymmetric extension. Comput. Phys. Commun. **108**, 56–74 (1998). arXiv:hep-ph/9704448
43. A. Djouadi, J. Kalinowski, M. Muehlleitner, M. Spira, HDECAY: Twenty$_{++}$ years after. Comput. Phys. Commun. **238**, 214–231 (2019). arXiv:1801.09506
44. A. Djouadi, J. Kalinowski, P.M. Zerwas, Two and three-body decay modes of SUSY Higgs particles. Z. Phys. C **70**, 435–448 (1996). arXiv:hep-ph/9511342
45. N.G. Deshpande, E. Ma, Pattern of symmetry breaking with two higgs doublets. Phys. Rev. D **18**, 2574–2576 (1978)
46. S. Nie, M. Sher, Vacuum stability bounds in the two Higgs doublet model. Phys. Lett. B **449**, 89–92 (1999). arXiv:hep-ph/9811234
47. B.W. Lee, C. Quigg, H.B. Thacker, Weak interactions at very high energies: the role of the higgs-boson mass. Phys. Rev. D **16**, 1519–1531 (1977)
48. B. Grinstein, C.W. Murphy, P. Uttayarat, One-loop corrections to the perturbative unitarity bounds in the CP-conserving two-Higgs doublet model with a softly broken $\mathbb{Z}_2$ symmetry. JHEP **06**, 070 (2016). arXiv:1512.04567
49. S. Kanemura, T. Kubota, E. Takasugi, Lee-Quigg-Thacker bounds for Higgs boson masses in a two doublet model. Phys. Lett. B **313**, 155–160 (1993). arXiv:hep-ph/9303263
50. A.G. Akeroyd, A. Arhrib, E.-M. Naimi, Note on tree level unitarity in the general two Higgs doublet model. Phys. Lett. B **490**, 119–124 (2000). arXiv:hep-ph/0006035
51. A. Arhrib, Unitarity constraints on scalar parameters of the standard and two Higgs doublets model, in Workshop on Noncommutative Geometry, Superstrings and Particle Physics Rabat, Morocco, June 16-17, 2000, (2000). arXiv:hep-ph/0012353
52. W. Grimus, L. Lavoura, O.M. Ogreid, P. Osland, A Precision constraint on multi-Higgs-doublet models. J. Phys. **G35**, 075001 (2008). arXiv:0711.4022
53. W. Grimus, L. Lavoura, O.M. Ogreid, P. Osland, The Oblique parameters in multi-Higgs-doublet models. Nucl. Phys. B **801**, 81–96 (2008). arXiv:0802.4353
54. Particle Data Group collaboration, M. Tanabashi, K. Hagiwara, K. Hikasa, K. Nakamura, Y. Sumino, F. Takahashi et al., Review of particle physics, Phys. Rev. D **98**, 030001 (2018)
55. D. Eriksson, J. Rathsman, O. Stal, 2HDMC: Two-Higgs-doublet model calculator physics and manual. Comput. Phys. Commun. **181**, 189–205 (2010). arXiv:0902.0851
56. ALEPH, DELPHI, L3, OPAL, LEP collaboration, G. Abbiendi et al., Search for Charged Higgs bosons: Combined Results Using LEP Data, Eur. Phys. J. **C73**, 2463 (2013). arXiv:1301.6065
57. Heavy Flavor Averaging Group (HFAG) collaboration, Y. Amhis et al., Averages of b-hadron, c-hadron, and τ-lepton properties as of summer (2014). arXiv:1412.7515
58. ATLAS collaboration, G. Aad et al., Search for charged Higgs bosons decaying via $H^{\pm} \to \tau^{\pm}\nu$ in fully hadronic final states using pp collision data at $\sqrt{s} = 8$ TeV with the ATLAS detector, JHEP **03**, 088 (2015). arXiv:1412.6663
59. CMS collaboration, V. Khachatryan et al., Search for a charged Higgs boson in pp collisions at $\sqrt{s} = 8$ TeV, JHEP **11**, 018 (2015). arXiv:1508.07774
60. ATLAS collaboration, G. Aad et al., Search for charged Higgs bosons in the $H^{\pm} \to tb$ decay channel in pp collisions at $\sqrt{s} = 8$ TeV using the ATLAS detector, JHEP **03**, 127 (2016). arXiv:1512.03704
61. F. Mahmoudi, SuperIso v2.3: A Program for calculating flavor physics observables in Supersymmetry. Comput. Phys. Commun. **180**, 1579–1613 (2009)
62. M. Misiak, M. Steinhauser, Weak radiative decays of the B meson and bounds on $M_{H^{\pm}}$ in the two-higgs-doublet model. Eur. Phys. J. C **77**, 201 (2017). arXiv:1702.04571
63. HFLAV collaboration, Y. Amhis et al., Averages of b-hadron, c-hadron, and τ-lepton properties as of summer 2016, Eur. Phys. J. **C77**, 895 (2017). arXiv:1612.07233